Cochlear mechanics with fluid viscosity and compressibility

P. Deepu*

Department of Mechanical Engineering, Indian Institute of Technology Patna, Bihta 801103, Bihar, India

(Received 27 December 2018; published 25 March 2019)

We extend the one-dimensional cochlear model to include the effect of viscosity and compressibility of the cochlear fluid. The resulting boundary-value problem is solved exactly using numerical techniques and semianalytically using the WKB approximation. Our results indicate the general trend of basilar membrane response increasing with an increase in compressibility or a decrease in viscosity. However, in the physiologically relevant range of these parameters, the change in the response is insignificant, justifying the assumption made in one-dimensional cochlear models that these effects are unimportant. Using the semianalytical WKB algorithm, we also demonstrate the simultaneous existence of forward- and backward-traveling waves on the basilar membrane.

DOI: 10.1103/PhysRevE.99.032417

I. INTRODUCTION

In mammalian auditory systems, the transduction of acoustic signals into neural signals occurs in the cochlea, a coiled duct filled with a fluid called perilymph. A flexible partition, called the cochlear partition, that runs along the length of the duct divides it into two chambers (see Fig. 1). The two chambers meet at a small opening at the apex of the cochlea called the helicotrema. The top chamber (scala vestibuli) opens to the middle ear through a membrane-covered opening called the oval window and the bottom chamber (scala tympani) through the round window. The cochlear partition houses an elastic membrane called the basilar membrane (BM). The ear drum and middle ear bones transmit the airborne acoustic vibrations to the oval window membrane, which in turn excites traveling pressure waves in the perilymph. The fluctuating pressure difference across the BM sets up traveling waves in the BM. The mechanical vibrations of the BM are converted to electrical signals by sensory hair cells residing on the BM.

Besides transduction, the cochlea is also responsible for the frequency analysis of the incoming sound waves. The mass, stiffness, and damping of the BM exhibit a spatial gradient causing the envelope of the surface waves elicited by a single tone sound wave (with stimulus frequency f and time period T) to peak at a resonant place which depends on f [1]. At the resonant place, the impedance of the BM is purely resistive and dissipates most of the energy of the traveling wave; Lighthill referred to this phenomenon as critical-layer absorption [2]. Thus specific exciting frequencies cause specific resonant places on the BM to respond and selectively stimulate the hair cells attached to the resonant place. This spatial mapping of frequency on the BM enables the brain to discriminate frequencies. The BM stiffness decays exponentially from the cochlear base to the apex [3] and hence the resonant places for higher (lower) frequencies are located near the cochlear base (apex), as can be seen in Fig. 2.

Understanding cochlear mechanics is not only of scientific interest, but also of technological importance in the diagnosis and treatment of hearing disorders. Much research effort has been aimed at constructing cochlear models. The pioneering mathematical model developed by Helmholtz [4] described the BM as an elastic sheet without any fluid interaction. This was followed by other theoretical models of varying degrees of complexity and focusing on various aspects of the problem. The simplest among these is the one-dimensional (1D) model which solves for the difference in the cross-sectionally averaged fluid pressures across the two chambers of the uncoiled cochlea and links it to the deflection of the BM through its impedance. This simple model has been very successful in accurately capturing the essential features of the BM vibration. Further, the model can be easily extended to simulate the active amplification of auditory stimuli mediated by the hair cells via a nonlinear feedback mechanism [5]. More sophisticated models consider the two-dimensional (see, e.g., [6–8]) and three-dimensional (see, e.g., [9,10]) versions of the problem.

We focus on how fluid viscosity and compressibility affect the results from the 1D cochlear model. Keller and Neu [11] concluded that viscosity is not important using asymptotic analysis in an open 2D model, where the fluid domains are unbounded. Most mathematical models consider the cochlear fluid to be inviscid based on the assumption that viscous effects are confined to narrow boundary layers near the cochlear walls and BM. Since the height of each chamber is of the order of 1 mm, it is unclear whether the results of Ref. [11] would apply to a real cochlea. Here we attempt to include the effect of fluid viscosity in the framework of a 1D model. Lighthill [2] suggested that fluid compressibility might affect the response at high frequencies, but no dedicated study had focused on this effect, specifically in 1D models.

We also revisit the WKB method of solving the cochlear model. Though it has been used to get closed-from solutions for 1D [12], 2D [13], and 3D [9] models, after making many approximations, a solution that is valid uniformly over the length of the cochlea is not yet available in the literature. Here

*deepu@iitp.ac.in

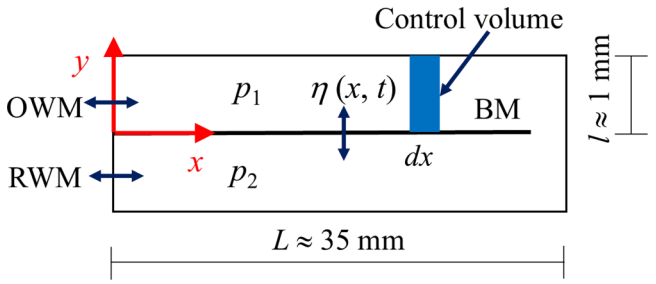

FIG. 1. Schematic diagram showing a longitudinal section of the uncoiled cochlea. BM: basilar membrane; OWM: oval window membrane; and RWM: round window membrane.

we adopt a semianalytical technique where the WKB solutions are integrated numerically. The motivation is twofold. First, it enables the relaxation of the assumptions made in previous studies with respect to the impedance of the BM. Most studies either completely neglect the resistive element of the impedance or assume it to be small in relation to the stiffness component so as to obtain closed-form solutions. This leads to a singular or near-singular behavior of the BM displacement near the resonant place and subsequently the WKB solution does not agree well with the exact solution in the regions apical to the resonant place. Without making any such assumptions, we achieve WKB solutions with global validity and accuracy. Second, this hybrid algorithm allows us to include the two linearly independent WKB solutions and provide insights into their relative importance. All the previous studies consider only the wave propagating in the forward direction (i.e., from the base to the helicotrema). This corresponds to only one of the WKB solutions. We show that the second mode is a backward-traveling wave with amplitude many orders of magnitude lower than the forward-traveling mode.

II. MODEL

We start deriving the modified 1D model by applying mass conservation on the upper chamber (see Fig. 1). We use the following notation: t is the time, x is the position along the BM, $u = (u, v)$ is the 2D fluid velocity field, p is the pressure, ρ is the fluid density, $\bar{\rho}$ is the mean fluid density, κ is the fluid compressibility (defined as the reciprocal of the bulk modulus $K = \bar{\rho}\frac{dp}{d\rho}$), $\omega = 2\pi f$ is the excitation angular frequency, L is the length of the BM, l is the height of each channel, $\eta(x, t)$ is the vertical displacement of the BM, $\eta_{\max}$ is the maximum displacement of the BM, λ is the wavelength of the BM wave, and the subscripts 1 and 2 denote upper and lower chambers, respectively. The continuity equation for the upper chamber reads

$$\frac{\partial \rho_1}{\partial t} + \bar{\rho}\nabla \cdot u_1 = 0. \tag{1}$$

Here the advective term in the material derivative of density is neglected since $O(u_1) \sim \omega\eta_{\max}$ and thus the order of magnitude of a typical advective term relative to that of the unsteady term is $O(u_1\frac{\partial \rho_1}{\partial x})/O(\frac{\partial \rho_1}{\partial t}) \sim \eta_{\max}/\lambda \ll 1$. Note that the 1D model is valid when the wavelength is long compared to the lateral dimensions of the chamber, thus the above inequality is highly satisfied. Introducing the fluid's compressibility, Eq. (1) becomes

$$\nabla \cdot u_1 = -\kappa\frac{\partial p_1}{\partial t}. \tag{2}$$

Since we seek a steady-state response of the BM to a single tone, the ansatz

$$u_1 = \tilde{u}_1(x)e^{i\omega t} + \text{c.c.} \tag{3}$$

(with similar expressions for other variables) is used to transform Eq. (2) from the time domain to the frequency domain as

$$\nabla \cdot \tilde{u}_1 = -\kappa i\omega\tilde{p}_1. \tag{4}$$

After integrating this equation over the differential control volume of height l and thickness dx located at x as shown in Fig. 1 and subsequently using the divergence theorem, we get

$$\frac{\partial \tilde{j}_1}{\partial x} - \tilde{V} = -i\omega\kappa l\tilde{p}_1. \tag{5}$$

Here $\tilde{j}_1 = l\tilde{u}_1$ is the longitudinal volume flow rate. Further, we have used the no-penetration boundary condition at the top wall of the chamber, i.e., $\tilde{v}_1(x, y = 0) = 0$, and the kinematic boundary condition at the BM, i.e., $\tilde{v}_1(x, y = l) = \tilde{V}$, the complex amplitude of the vertical velocity of the BM. The vertical displacement of the BM is driven by the pressure difference across the BM $p = p_1 - p_2$ according to the equation

$$m(x)\frac{\partial^2\eta}{\partial t^2} + r(x)\frac{\partial\eta}{\partial t} + k(x)\eta = -p, \tag{6}$$

where $m(x)$, $r(x)$, and $k(x)$ denote the mass, resistance, and stiffness per unit area of the BM. The negative sign indicates that a higher pressure in the lower chamber causes a positive BM displacement. In the frequency domain, this equation leads to

$$\tilde{V} = -\tilde{p}/Z, \tag{7}$$

where

$$Z(x) = i\omega m(x) + r(x) - i\frac{k(x)}{\omega}, \tag{8}$$

is the impedance per unit area of the BM. In this paper we use $m(x) = 0.5$ kg/m^2, $k(x) = 1 \times 10^{10}e^{-300x}$ N/m^3, and $r(x) = 3 \times 10^4 e^{-150x}$ N s/m^3, where x is in meters [6].

Note that the resistance $r(x)$ accounts mainly for the structural damping of the BM (of the cochlear partition, to be more precise). Direct damping of BM oscillations due to viscous drag force from the perilymph is expected to be insignificant for small amplitude of vibrations. This is because the tangential viscous stresses act on both sides of the BM along in the x direction and thus do not affect the transverse motion in the y direction. However, as we will see later, at high enough fluid viscosity, the viscous dissipation in the fluid reduces the energy available for the BM excitation and thus in turn decreases the BM response. In passing, we remark that active cochlear models exist which incorporate a negative damping of the BM in the region basal to the resonant place [14], in an attempt to represent the active behavior of hair cells, e.g., hair-bundle motility [15]. Such an active BM pumps energy (rather

than dissipating energy) into the cochlear wave and thus helps to explain the mechanism of cochlear amplification. In the present work we focus on the macromechanics of a passive cochlea and do not consider such an active phenomenon.

Now let us consider the linearized 1D momentum equation for the fluid in the top chamber

$$\bar{\rho}\frac{\partial u_1}{\partial t} = -\frac{\partial p_1}{\partial x} - \frac{2\mu}{l^2}u_1. \tag{9}$$

Here μ denotes the dynamic viscosity of the cochlear fluid. The last term represents the viscous force per unit volume of the fluid and its functional dependence on the average velocity u_1 can be easily obtained by scaling analysis. The prefactor 2 in the scaling arises from a comparison with the solution of plane Poiseuille flow; however, the actual value of the prefactor does not matter in the present analysis as long as it is of order 1. After transforming Eq. (9) to the frequency domain and multiplying by l gives

$$i\omega\bar{\rho}\tilde{j}_1 = -l\frac{\partial \tilde{p}_1}{\partial x} - \frac{2\mu}{l^2}\tilde{j}_1. \tag{10}$$

Using Eqs. (7) and (10) in Eq. (5) yields

$$\frac{\partial^2 \tilde{p}_1}{\partial x^2} + \omega^2\bar{\rho}\kappa\left(1 - i\frac{2\mu}{l^2\omega\bar{\rho}}\right)\tilde{p}_1 - \frac{i\omega\bar{\rho}}{Z(x)l}\left(1 - i\frac{2\mu}{l^2\omega\bar{\rho}}\right)\tilde{p} = 0. \tag{11}$$

Repeating the steps for the lower chamber leads to

$$\frac{\partial^2 \tilde{p}_2}{\partial x^2} + \omega^2\bar{\rho}\kappa\left(1 - i\frac{2\mu}{l^2\omega\bar{\rho}}\right)\tilde{p}_2 + \frac{i\omega\bar{\rho}}{Z(x)l}\left(1 - i\frac{2\mu}{l^2\omega\bar{\rho}}\right)\tilde{p} = 0. \tag{12}$$

Subtracting Eq. (12) from Eq. (11), we get

$$\frac{\partial^2 \tilde{p}}{\partial x^2} + q^2(x)\tilde{p} = 0, \tag{13}$$

where

$$q^2(x) = \left[\omega^2\bar{\rho}\kappa - \frac{2i\omega\bar{\rho}}{Z(x)l}\right]\left(1 - i\frac{2\mu}{l^2\omega\bar{\rho}}\right). \tag{14}$$

III. RESULTS AND DISCUSSION

Note that setting κ and μ equal to 0 in Eq. (13) recovers the second-order wave equation for the pressure difference considered in previous studies [16]. Combined with the no-pressure-difference boundary condition at the helicotrema, i.e., $\tilde{p}(L) = 0$, Eq. (13) can be solved for $\tilde{p}$ with various sound pressure levels (SPLs) (from [5]) at the cochlea base, $\tilde{p}(0)$. The boundary-value problem is solved numerically (for details see [5]) and using a hybrid WKB numerical approach.

The WKB approach gives the following asymptotic solution, the validity of which will be discussed later:

$$\tilde{p}(x) = \frac{C_+}{\sqrt{q(x)}}\exp\left(+i\int_0^x q(\xi)d\xi\right) + \frac{C_-}{\sqrt{q(x)}}\exp\left(-i\int_0^x q(\xi)d\xi\right). \tag{15}$$

We call the first term in Eq. (15) the plus mode and the second term the minus mode. In previous studies, WKB solutions are found to show only local agreement with the exact solutions; a significant difference is observed between the solutions both quantitatively and qualitatively in the region apical to the BM resonant peak. To be more specific, the WKB response drops much more steeply in the downward sloping portion of the response compared to the exact solution (see, e.g., Figs. 2 and 3 in Ref. [17]). Here we consider the linear combination of the two WKB solutions as the general solution to Eq. (13). Previous studies invariably consider only the forward-traveling solution [the minus mode, the second term in Eq. (15)], based on the observation that waves on the BM travel only in one direction [1,13]. As already explained, the waves emanating from the cochlea base travel toward the apex and get absorbed near the resonant place. In accordance with this physical picture, the waves cannot travel beyond the resonant place. These studies however put restrictions on the BM impedance (e.g., the resistive component is neglected or considered to be small [12]) so as to get a closed-form solution of the integral. Here we seek to understand the role of the second mode (referred to as the plus mode hereafter) without any assumptions as made in the previous studies; thus we need to resort to numerical integration for the solution of Eq. (15). Also note that by considering only one of the modes, the solution can satisfy only one of the boundary conditions, namely, the one at the cochlea base. Here, by considering a superposition of both linearly independent solutions, both boundary conditions are incorporated. Thus we have

$$C_+ = \frac{\tilde{p}(0)\sqrt{q(0)}}{1 - e^{i2H}}, \quad C_- = \frac{\tilde{p}(0)\sqrt{q(0)}e^{i2H}}{e^{i2H} - 1}, \tag{16}$$

where $H = \int_0^L q(\xi)d\xi$. The exact solution and the WKB solution constructed herein show global agreement with each other (Fig. 2), underscoring the accuracy and uniform validity of Eq. (15).

However, the quantitative agreement is less impressive at low frequencies. For instance, the deviation of the peak amplitude in the WKB solution from the exact solution is about 7% for $f = 1000$ Hz and 74% for $f = 100$ Hz. This is expected because the validity of the WKB approximation becomes questionable at long wavelengths. The WKB approximation is valid when the coefficient $q^2(x)$ in the differential equation (13) is a slowly varying function [17] or, more precisely, when $|\frac{dq}{dx}| \ll q^2$. Since $q^2(x)$ is related to the impedance of the cochlear partition [Eq. (14)], $|\frac{dq}{dx}|$ can be crudely considered as the rate of change of the impedance. Also note that $q(x)$ can be interpreted as the local wave number of the cochlear waves (solutions to the differential equation), as can be seen from Eq. (15). Introducing the local wavelength [$\lambda(x) = \frac{2\pi}{q(x)}$], the above condition can be recast as

$$\left|\frac{dq}{dx}\right|\lambda \ll 2\pi q. \tag{17}$$

In simple terms, this means that the variation of impedance over a wavelength of the traveling wave should be small. As can be seen from Figs. 2(c) and 2(d), at lower frequencies the wavelength near the cochlea base is larger; hence the above validity criterion becomes increasingly unsatisfied, which explains the greater disagreement between the WKB solution and the exact solution.

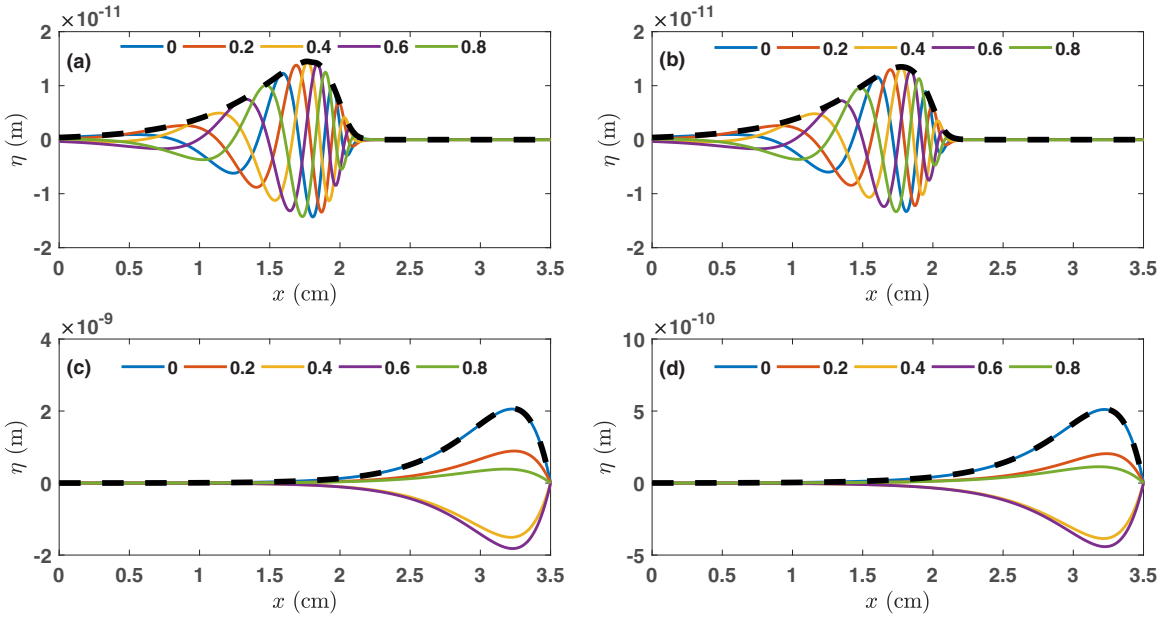

FIG. 2. Instantaneous waves (solid line) and wave envelope (dashed line) on the BM for (a) and (b) $f = 1$ kHz and (c) and (d) $f = 20$ Hz: (a) and (c) exact solution and (b) and (d) WKB approximation. Instantaneous waves are shown at uniformly spaced time instants over a period of oscillation. The time instants normalized by the period of oscillation T are indicated in the legends. The parameter values are $L = 35$ mm and $l = 1$ mm from [5], $\bar{\rho} = 1000$ kg/m^3 from [6], $\mu = 0$, $\kappa = 0$, and a SPL of 40 dB. Note the shift in the location of the peak amplitude toward the apex of the BM at the lower frequency. The location of the resonant place is $x \approx 1.7$ cm for $f = 1$ kHz and $x \approx 3.2$ cm for $f = 20$ Hz.

The excellent agreement between the WKB solutions considering a superposition of the two modes [Eq. (15)] and the exact solution raises the question of how the single-forward-traveling-wave solution reported previously yields the correct result. To answer this question, we present the magnitude of each of the modes in Fig. 3 and observe that the plus mode is several orders of magnitude lower in magnitude than the minus mode. The reason for this is that e^{i2H} is an exponentially large number. For instance, for the parameter values used in Fig. 3, $|e^{i2H}| \sim O(10^{30})$. It is a simple exercise to show that in the limit of $|e^{i2H}| \to \infty$, Eq. (15) reduces to

$$\tilde{p}(x) = \frac{\tilde{p}(0)\sqrt{q(0)}}{\sqrt{q(x)}} \exp\left(-i\int_0^x q(\xi)d\xi\right), \tag{18}$$

which is the WKB solution considering only the minus mode. Now it becomes clear as to why ignoring the backward-traveling wave does not affect the accuracy of the overall solution. Nevertheless, our analysis shows that both modes exist simultaneously, albeit the backward-traveling wave is minuscule in magnitude relative to the forward-traveling wave.

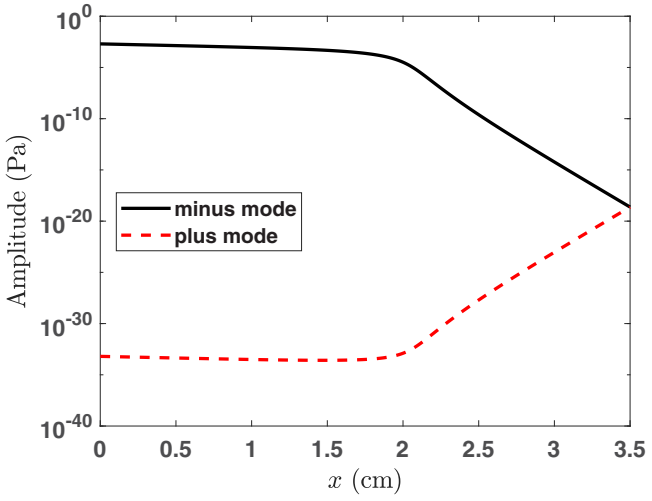

FIG. 3. Amplitude of the two WKB modes in Eq. (15) for $f = 1$ kHz, a SPL of 40 dB, $\mu = 0$, and $\kappa = 0$. Note the *smallness* of the plus mode.

Now we present the effect of variation in fluid viscosity and compressibility in Figs. 4 and 5, respectively, at different frequencies and sound intensities. We change each of these fluid properties over 6 orders of magnitude around their respective values relevant for mammalian cochleae [$\mu \sim O(10^{-3})$ Pa s [6] and $\kappa \sim O(10^{-9})$ m^2/N [18]]. Figure 4 shows that the BM response decreases with an increase in μ for a given SPL. This is expected because the energy loss due to viscous dissipation in the fluid during one period of oscillation of the BM displacement scales as

$$E_v \sim \mu \eta_{\max}^2 \omega l, \tag{19}$$

which is proportional to μ. Thus, for a fixed input energy at the stapes, the energy available for sustaining the BM oscillations will decrease as viscosity increases.

However, as can be seen from Fig. 4, the effect of viscous dissipation affects the BM displacement only at large values of μ. At $\mu \sim O(10^{-3})$ Pa s, the BM response has plateaued at its value corresponding to $\mu = 0$. The weak dependence of the local wave number on μ at low μ is clear from Eq. (14); when $\mu \ll l^2\omega\bar{\rho}$, the effect of viscosity is expected to be negligible.

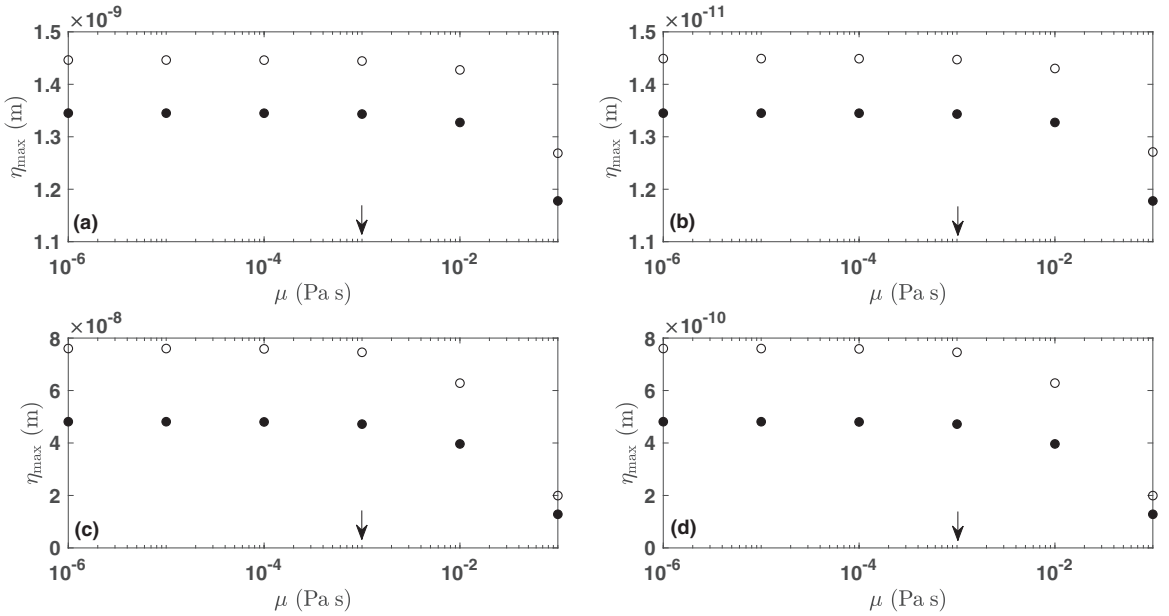

FIG. 4. Effect of fluid viscosity on the peak amplitude of BM displacement for (a) $f = 1000$ Hz and a SPL of 80 dB, (b) $f = 1000$ Hz and a SPL of 40 dB, (c) $f = 100$ Hz and a SPL of 80 dB, and (d) $f = 100$ Hz and a SPL of 40 dB. Open symbols denote exact solutions and closed symbols WKB solutions. Here $\kappa = 0$. The black arrow indicates roughly the value of fluid viscosity that is relevant to mammalian cochleae.

Further, at $f = 1$ kHz, this condition becomes $\mu \ll O(1)$ Pa s and at $f = 100$ Hz, $\mu \ll O(0.1)$ Pa s; this explains why the change in BM response with μ is higher at $f = 100$ Hz than at $f = 1$ kHz. Similar arguments hold for compressibility (Fig. 5). For the same input energy (as dictated by the SPL) and excitation frequency, higher values of κ translate to a higher fluid deformation rate and higher pressure difference fluctuations across the BM and thus higher BM response. The other qualitative trends observed in Figs. 4 and 5, such as an increase in BM response with an increase in the SPL and a decrease in excitation frequency, are physically consistent with the characteristics of a linear oscillator.

IV. CONCLUSION

Our results show that in 1D cochlear models the effect of viscosity and compressibility can be safely ignored. Changes in μ and κ cause any substantial change in the BM response

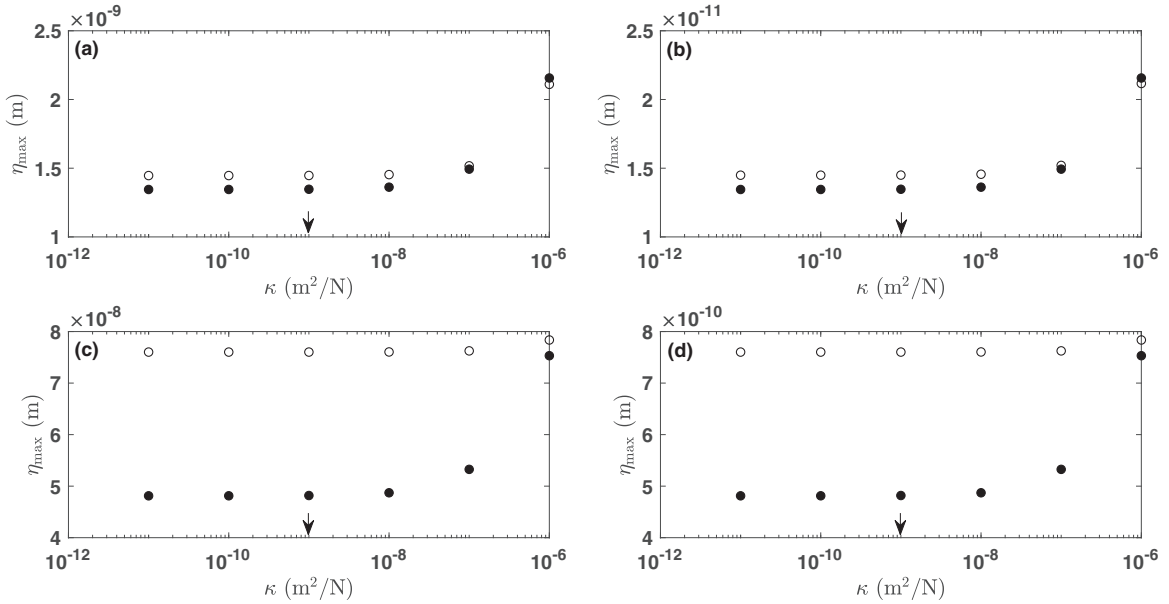

FIG. 5. Effect of fluid compressibility on the peak amplitude of BM displacement for (a) $f = 1000$ Hz and a SPL of 80 dB, (b) $f = 1000$ Hz and a SPL of 40 dB, (c) $f = 100$ Hz and a SPL of 80 dB, and (d) $f = 100$ Hz and a SPL of 40 dB. Open symbols denote exact solutions and closed symbols WKB solutions. Here $\mu = 0$. The black arrow indicates roughly the value of fluid compressibility that is relevant to mammalian cochleae.

or the location of peak amplitude (data not shown) only at large values of μ and κ. The above conclusions are expected to apply to mammalian cochlear models in general, since μ and κ of the cochlear fluid are not expected to be very different.

We also explored the role of the usually ignored second (backward-traveling) WKB mode. Since the 1D model is described by a second-order wave equation, the general solution obtained by the superposition of the two linearly independent waves was examined. Numerical results demonstrate that the backward-traveling wave is negligible compared to the forward-traveling wave. Thus the present study shows that the total WKB solution to the 1D model is in fact a superposition of a large forward-traveling wave and a negligibly small backward-traveling wave. This explains why only one linearly independent solution provides the correct results to the boundary-value problem.

Note that the two waves considered here are not the dual traveling waves studied in the context of a two-degree-of-freedom model [19]. The semianalytical approach also shows that the WKB solutions possess a uniform accuracy (over the length of the cochlea) for realistic impedance variations (without any assumptions such as small damping) across a wide range of frequencies and sound pressure levels. The coexistence of two waves propagating in opposite directions on the BM suggests that the cochlear waves could undergo internal reflections, a finding that is relevant to the poorly understood phenomenon of otoacoustic emission. Otoacoustic emissions are sounds generated by the inner ear (in the presence or absence of external stimulation) and are believed to be produced from the reflection of cochlear traveling waves by random irregularities in the impedance of the cochlea [20]. Understanding the implications of coexisting forward- and backward-traveling waves, induced by harmonic excitation of the stapes, for the mechanism of evoked otoacoustic emissions is left as a future task.

[1] G. Von Békésy and E. G. Wever, *Experiments in Hearing* (McGraw-Hill, New York, 1960), Vol. 8.

[2] J. Lighthill, J. Fluid Mech. **106**, 149 (1981).

[3] G. Emadi, C.-P. Richter, and P. Dallos, J. Neurophysiol. **91**, 474 (2004).

[4] H. Helmholtz, *On the Sensations of Tone* (Courier, Chelmsford, 2013).

[5] T. Duke and F. Jülicher, Phys. Rev. Lett. **90**, 158101 (2003).

[6] M. Lesser and D. Berkley, J. Fluid Mech. **51**, 497 (1972).

[7] R. P. Beyer, Jr., J. Comput. Phys. **98**, 145 (1992).

[8] C. Pozrikidis, J. Fluids Struct. **24**, 336 (2008).

[9] L. A. Taber and C. R. Steele, J. Acoust. Soc. Am. **70**, 426 (1981).

[10] E. Givelberg and J. Bunn, J. Comput. Phys. **191**, 377 (2003).

[11] J. B. Keller and J. C. Neu, J. Acoust. Soc. Am. **77**, 2107 (1985).

[12] G. Zweig, R. Lipes, and J. Pierce, J. Acoust. Soc. Am. **59**, 975 (1976).

[13] C. R. Steele and C. E. Miller, J. Acoust. Soc. Am. **68**, 147 (1980).

[14] E. De Boer, J. Acoust. Soc. Am. **73**, 567 (1983).

[15] B. Sul and K. H. Iwasa, Biophys. J. **97**, 2653 (2009).

[16] G. Ni, S. J. Elliott, M. Ayat, and P. D. Teal, BioMed Res. Int. **2014**, 150637 (2014).

[17] E. De Boer and M. Viergever, Hear. Res. **8**, 131 (1982).

[18] R. Z. Gan, B. P. Reeves, and X. Wang, Ann. Biomed. Eng. **35**, 2180 (2007).

[19] J. S. Lamb and R. S. Chadwick, Phys. Rev. Lett. **107**, 088101 (2011).

[20] G. Zweig and C. A. Shera, J. Acoust. Soc. Am. **98**, 2018 (1995).